

# A Reconfigurable Dual Band LTE Small Cell RF Front-end/Antenna System to Support Carrier Aggregation

Cyril Jouanlanne<sup>1,2</sup>, Christophe Delaveaud<sup>1,2</sup>(✉),  
Yolanda Fernández<sup>3</sup>, and Adrián Sánchez<sup>3</sup>

<sup>1</sup> Univ. Grenoble-Alpes, Grenoble, France

{cyril.jouanlanne, christophe.delaveaud}@cea.fr

<sup>2</sup> CEA, LETI, MINATEC Campus, 17 rue des Martyrs, 38054 Grenoble, France

<sup>3</sup> TTI, PCTCAN, C/Albert Einstein 14, 39011 Santander, Spain

{yfernandez, asanchez}@ttinorte.es

**Abstract.** In this contribution, the prototype of an energy efficient RF front-end combined to a miniaturized highly efficient antenna system is presented. This demonstrator is designed for LTE small cell base station applications and can address both LTE band 7 & 20. It supports carrier aggregation (CA) for capacity network improvement and is compatible with inter-band CA as well as contiguous and non-contiguous intra-band CA. The measurement results show an energy consumption saving of around 30 % and a size reduction factor of 3 for the antenna system compared to regular base station antennas. The proposed design demonstrates the possibility of increasing the energy efficiency as well as the level of integration of a small cell base station despite the use of new technology enablers such as CA technique.

**Keywords:** Carrier aggregation · Multi-band antennas · Reconfigurable solutions · Energy efficiency

## 1 Introduction

One of the key aspects in future network deployments is the increasing bandwidth demand in confrontation with spectrum availability. ITU has proposed the technique of carrier aggregation (CA) supporting up to 100 MHz system bandwidth for LTE-Advanced (LTE-A) [1]. This technique enables aggregation of multiple component carriers (CCs) providing operators the maximum flexibility for using their available spectrum. Therefore LTE-A provides much higher throughputs than otherwise possible with the potential of achieving more than 1 Gb/s throughput for downlink (DL) and 500 Mb/s throughput for uplink (UL).

Three different CA modes are defined: intra-band contiguous CA (CCs are contiguous within the same band), intra-band non-contiguous CA (CCs are non-contiguous in the same band) and inter-band CA (CCs are in different bands).

To handle bandwidths up to 100 MHz in different frequency bands, innovative solutions are required for antenna and RF front-end. Concerning the antenna solution, the focus is on the bandwidth optimization enabling antenna miniaturization. Thus, the

antenna system instantaneous bandwidth has been reduced to the minimum in order to miniaturize the antenna size without impacting its performance. Frequency agility technique has been used to compensate this bandwidth reduction by giving the ability to the antenna to reconfigure its frequency bandwidth according to the active CA configuration. This technique has been so far mainly used in handset antenna design for CA purposes as demonstrated in [2]. On the topic of RF front-ends, reconfigurable solutions in terms of bandwidth and frequency of operation are demanded. However, peak-to-average power ratio (PAPR) is an important issue in CA, because CC aggregation causes an increase in PAPR. For the DL, the eNB should afford the PAPR increase caused by multiple CCs.

This paper addresses the issue of two innovative reconfigurable solutions to support CA. One solution is a multi-band frequency agile antenna which is able to adjust its bandwidth according to the active CA configuration. As well as a reconfigurable RF front-end capable to work at different operating points to improve energy efficiency depending on CA configuration.

For experimental validation, the proposed scenario is a small cell base station supporting intra-band CA in LTE band 7 (2620–2690 MHz) and inter-band CA in LTE band 20 (791–821 MHz) & LTE band 7 (2620–2690 MHz).

This work is structured as follows: Sect. 2 describes the multi-band frequency agile antenna. Section 3 presents the reconfigurable RF front-end. Section 4 depicts the small cell reconfigurable carrier aggregation demonstrator. Finally, Sect. 5 concludes the paper, highlighting the main results.

## 2 Multi-band Frequency Agile Antenna

A dual band (LTE band 7 & band 20) dual access frequency agile antenna system capable to adapt its frequency bandwidth to the active CA configuration has been developed. Frequency agility is used to reduce the antenna instantaneous bandwidth which enables miniaturization without performance reduction.

### 2.1 Design

Due to its low operating frequency bandwidth, only band 20 antenna requires a miniaturization. Based on the fact that the size of an antenna is proportional to its bandwidth [3, 4], the main idea with this antenna design is to do the miniaturization by limiting the frequency bandwidth to a single band 20 sub-channel instead of the whole band 20, reducing the instantaneous bandwidth from 70 MHz to twice 10 MHz. Thus, the antenna has been made dual resonant with two very narrow closely spaced resonances and the frequency agility technique has been used to tune the antenna resonances at the right frequency according to the active CA configuration.

The antenna system (Fig. 1) is based on two microstrip patch antennas, one covering LTE band 7 and the other one LTE band 20. Band 20 antenna is miniaturized thanks to classical loading and folding techniques. Both antennas are co-located on a square  $100 \times 100 \text{ mm}^2$  ground plane and the antenna system only takes up a small

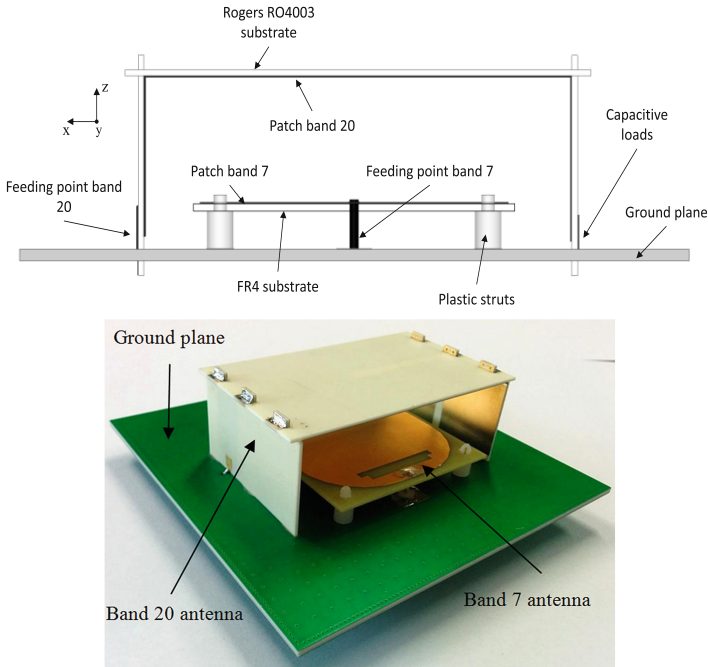


**Fig. 1.** Drawing and picture of the antenna prototype.

volume of  $66 \times 54.5 \times 23 \text{ mm}^3$  ( $\lambda_0/5.7 \times \lambda_0/7 \times \lambda_0/16.5$  with  $\lambda_0 = 379 \text{ mm}$  @791 MHz).

This mechanical arrangement with band 20 antenna right above band 7 antenna is possible due to their orthogonal polarizations as well as the fact that their respective strong near field spots are distinct and do not interfere significantly. This aspect is developed and illustrated in [5].

Two digitally tunable capacitors (DTCs) are used as frequency agility active components in this design. DTCs have been selected due to their superior linearity performance compared to other tuning components such as varactor diodes. They are also very easy to use and only require a SPI bus to control their effective capacitance.

## 2.2 Performance Evaluation

A measurement campaign was carried out to evaluate the antenna system electrical and radiated characteristics.

Figure 2 shows the reflection coefficient (S11) at the antenna system band 20 and band 7 ports. A reflection coefficient below -10 dB (worst case -7.7 dB) for band 20 and -12 dB for band 7 is achieved whichever the antenna state. A very good agreement is obtained between simulated and measured reflection coefficient in band 7. The comparison is equally good in band 20. The more visible discrepancies reflect very little difference due to low values shown with a logarithmic scale.

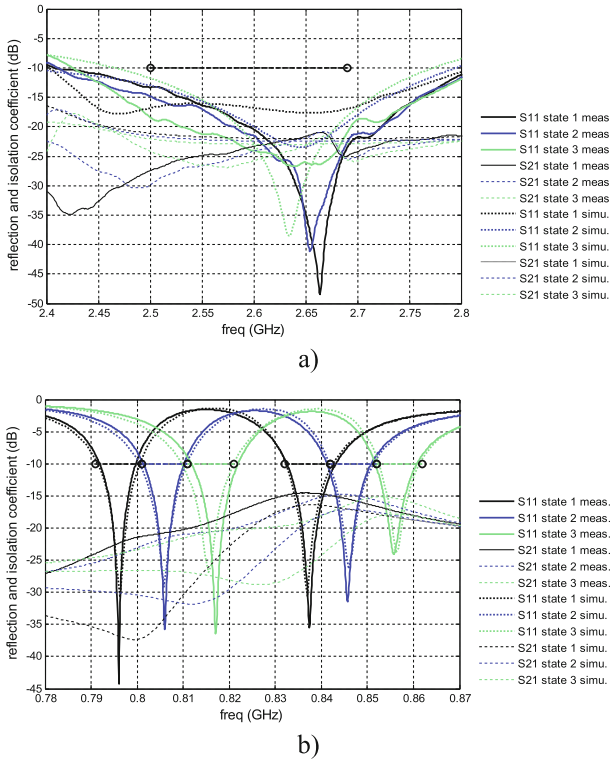


**Fig. 2.** Measured and simulated reflection coefficients at band 20 (a) and band 7 (b) RF ports and isolation between both RF ports for different DTC states.

Similar remark can be made with the isolation parameters (S21) that are close in simulation and measurement. An isolation level higher than 14.5 dB within band 20 and 20 dB within band 7 is demonstrated between both RF ports for the three states. This level of isolation will ensure a good electromagnetic compatibility between both antennas.

A peak realized gain (computed over two orthogonal elevation planes) better than 3 dBi for band 20 and 8 dBi for band 7 (Fig. 3) has been measured. These gain levels will ensure the good connectivity of the small cell base station.

The antenna system frequency agility is also demonstrated in Figs. 2 and 3, where the band 20 antenna ability to tune its frequency bandwidth in order to cover the three band 20 sub-channels is shown.

Realized gain patterns of band 20 antenna (Fig. 4) show that the main beam is oriented towards the Z + axis ( $\pm 10^\circ$ ) at both frequencies. The size of the ground plane being about  $\lambda_0/4$ , it is too small to ensure its reflector role. Therefore, the back radiation is relatively high (front to back ratio of about 3 dBi) and the directivity is consequently limited. Realized gain patterns of band 7 antenna (Fig. 5) show that the main beam is oriented towards the Z + axis ( $\pm 10^\circ$ ). Due to the sufficient size of the ground plane,

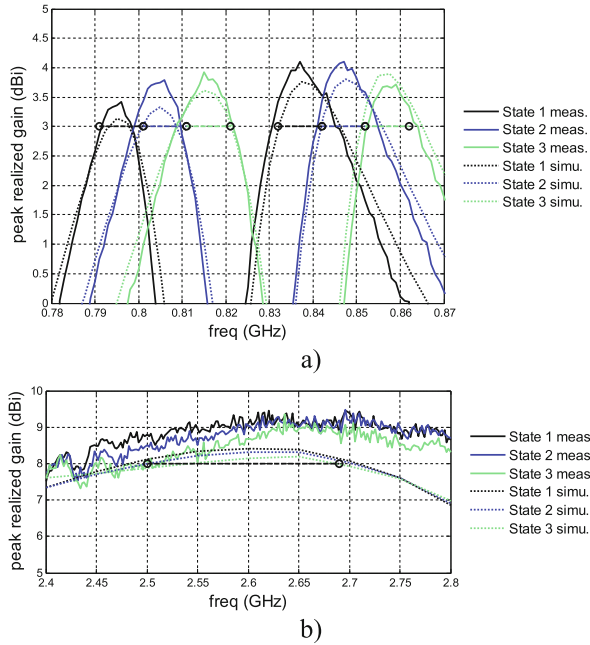


**Fig. 3.** Measured and simulated peak realized gain of band 20 (a) and band 7 (b) antennas for different DTC states.

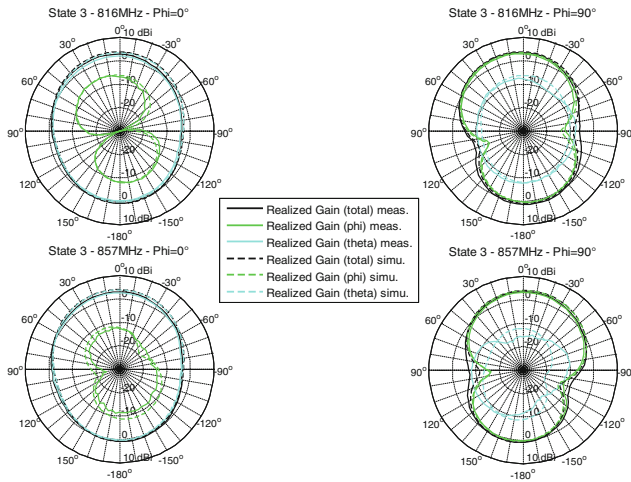


**Fig. 4.** Measured and simulated realized gain pattern of band 20 antenna.

there is almost no radiation towards the Z- hemisphere meaning a good front to back ratio (greater than 15 dB). This kind of radiation pattern was targeted in order to have the best performance once the base station located against a wall for instance.

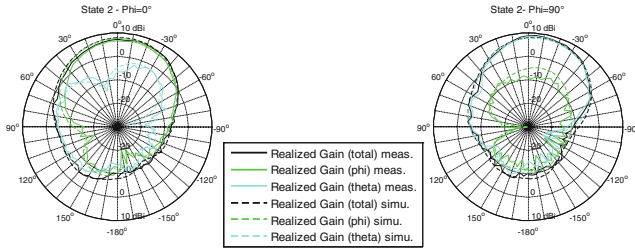


Fig. 5. Measured and simulated realized gain pattern of band 7 antenna.

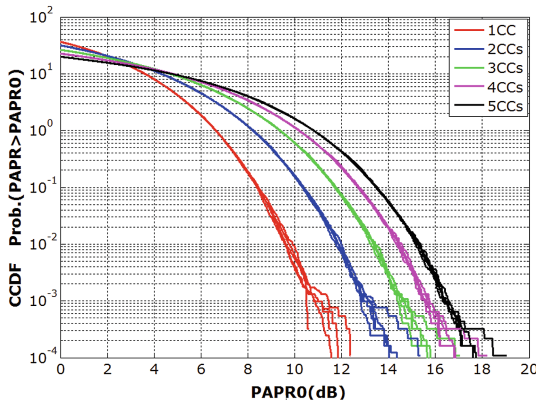


Fig. 6. CCDF simulation results from 1CC to 5CCs using E-TM1.1.

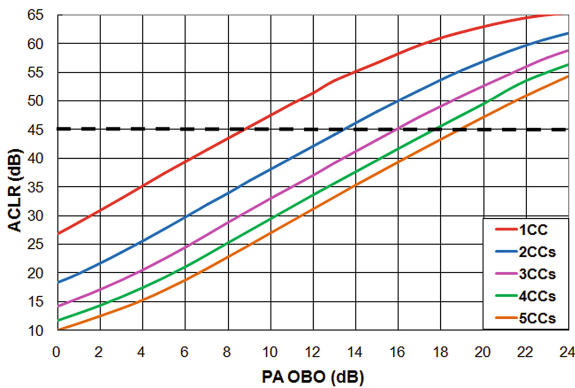


Fig. 7. ACLR simulated results vs PA OBO from 1CC to 5CCs using E-TM1.1 supporting intra-band contiguous CA.

### 3 Reconfigurable RF Front-end

A reconfigurable RF front-end capable to adapt to different CA configurations with different number of aggregated CCs providing energy savings has been developed. The solution is based on a reconfigurable power amplifier (PA) working at different operating points which provides optimized output power levels for CA.

#### 3.1 Design

To support different CA configurations with different number of aggregated CCs, base station transmitter specifications [6] were considered in order to define mainly PA requirements. Depending on the number of aggregated CCs and CA configuration, different output back-off (OBO) levels at PA are required related to PAPR requirements. To calculate OBO specification, it is normally sufficient to apply 0.01 % complementary cumulative distribution function (CCDF) of the waveform [7]. CCDF characterizes the weighted probability of the signal excursions that lead to distortions, by indicating the number of samples where the signal peak power exceeds its average power by a certain value. CC aggregation causes an increase in PAPR due to the influence of aggregated CCs on the unwanted emissions and particularly on adjacent channel leakage power ratio (ACLR), which should be at least 45 dB.

To evaluate technical specifications, E-UTRA test models [8] are defined. E-UTRA test model 1.1 (E-TM1.1) verifies most PA specifications.

Firstly, simulations merging from 2CCs to 5CCs were carried out to evaluate LTE-A waveform and characterize its CCDF curves (Fig. 6). These simulations were performed with bandwidths from 3 MHz to 20 MHz, showing slight variations.

Furthermore, the OBO impact over ACLR specification was evaluated. Several simulations were performed modifying the OBO at the PA in order to determine the 45 dB ACLR threshold. Figure 7 presents the ACLR simulated results depending on the PA OBO from 1CC to 5CCs using E-TM1.1 supporting intra-band contiguous CA.

Table 1 summarizes the simulated results by combining the 0.01 % waveform CCDF evaluation and the ACLR evaluation to support intra-band contiguous CA from 1CC to 5CCs. Total OBO requirement must be the most restrictive value between both simulations.

**Table 1.** OBO requirements to support intra-band contiguous CA from 1CC to 5CCs.

Intra-band contiguous CA	OBO requirement		
	0.01 % CCDF evaluation	45 dB ACLR evaluation	Global evaluation
1 CC	9.6 dB	8.7 dB	9.6 dB
2 CCs	11.8 dB	13.4 dB	13.4 dB
3 CCs	13.3 dB	15.9 dB	15.9 dB
4 CCs	14.3 dB	17.7 dB	17.7 dB
5 CCs	15.2 dB	18.9 dB	18.9 dB

As shown in Table 1, the higher the number of CCs is, the higher is the impact of ACLR specification over OBO requirement.

The study was also extended to intra-band non-contiguous CA. It was checked that increasing the gap among CCs, OBO requirement reduces mainly owing to a lower impact of ACLR specification. For instance, in case of having 2CCs with a gap between CCs equal to the bandwidth, OBO requirement decreases to 12.6 dB. With a gap of twice the bandwidth, it reduces up to 11.8 dB.

### 3.2 Prototype

To validate the PA OBO requirement analysis for different CA modes, a reconfigurable RF front-end was developed (Fig. 8). It supports intra-band CA allowing up to 3CCs in LTE band 7 and inter-band CA in LTE band 20 & band 7. The hardware prototype is composed of three modules: the signal generation module, the RF gain block module and the reconfigurable PA capable to work at different operating points to optimize CA energy efficiency performance.



**Fig. 8.** Picture of the reconfigurable RF front-end prototype.

The signal generation module translates LTE baseband signals (E-UTRA test models) into LTE band 20 & band 7 RF signal, acting as an up-converter/modulator. Three RF signals are generated at tuning frequencies and appropriately combined using two RF splitters and one RF switch to configure different CA configurations. The RF gain module amplifies the RF signals from the signal generation module, also includes a digital attenuator to adjust the output power level to ease the characterization of the reconfigurable PA. Finally, the reconfigurable PA for LTE band 7 is integrated.

A console has been designed to configure different CA configurations defining the operating frequencies and the number of aggregated CCs.

The commercial PA, AFT20S015 N from Freescale, was implemented as the reconfigurable PA to validate the proposed solution. Its 1 dB compression output power (P1 dB) is about 38 dBm at 28 V drain voltage. Moreover, it was tested at drain voltages from 28 V to 14 V (Fig. 9).

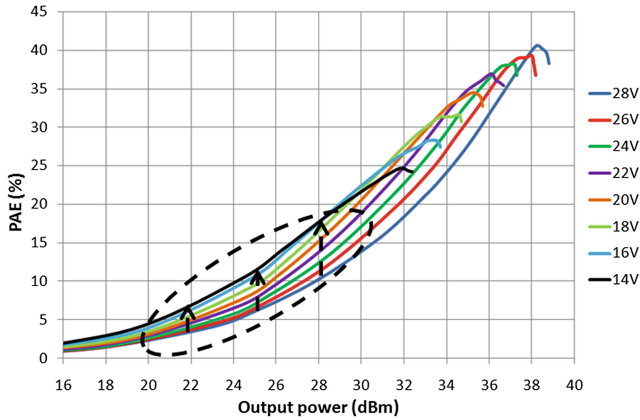


Fig. 9. PAE results in AFT20S015 N for different operating points.

The higher the drain voltage is, the higher is the possible delivered output power level. Nevertheless, depending on CA configuration there is an operating point optimized to deliver the required output power improving EE compared to single operating point as shown Fig. 9.

### 3.3 Performance Evaluation

For proof-of-concept validation, the most restrictive CA mode evaluated with the prototype is 3CCs in intra-band contiguous CA configuration, which requires 15.9 dB OBO. Considering 38 dBm P1 dB for 28 V drain voltage and aggregating 3CCs there is an increase in 4.7 dB in the average power due to the grouping. Therefore it can assume about 17 dBm as the average power per CC. Table 2 presents the associated operating points and the power-added efficiency (PAE) enhancement for different CA configurations. The evaluation was completed for intra-band contiguous CA up to 3CCs and for intra-band non-contiguous CA merging 2CCs with a gap equal to the bandwidth and twice the bandwidth.

For 1CC of 17 dBm average power and 9.6 dB OBO requirement, 16 V operating point is enough, providing 50 % PAE enhancement as shown Table 2. For 2CCs, the average output power is 20 dBm and different OBO requirements are associated to different CA configurations which can be fulfilled using different operating points, providing between 25 % and 39 % PAE enhancement.

## 4 Reconfigurable CA Demonstrator

A demonstrator combining the antenna system and the RF front-end was realized showing the compatibility between both subsystems.

The interfaces between the multi-band frequency agile antenna and the reconfigurable RF front-end are SMA connectors, one for each frequency band. Therefore RF

**Table 2.** Energy efficiency evaluation for different CA configurations.

CA configuration	PA OBO (dB)	Operating point (V)	Output power (dBm)	PAE (%)	PAE enhancement (%)
1 CC	9.6 dB	28 V	27.3 dBm	9.4 %	50 %
		16 V	17.9 dBm	2.8 %	
		28 V		1.4 %	
2 CCs non-contiguous (Gap = 2*Bandwidth)	11.8 dB	28 V	22.7 dBm	3.9 %	39 %
		20 V	17.1 dBm	1.8 %	
		28 V		1.1 %	
2 CCs non-contiguous (Gap = Bandwidth)	12.6 dB	28 V	21.6 dBm	3.3 %	35 %
		21 V	16.9 dBm	1.7 %	
		28 V		1.1 %	
2 CCs contiguous	13.4 dB	28 V	21.2 dBm	3 %	25 %
		22 V	17.4 dBm	1.6 %	
		28 V		1.2 %	
3 CCs contiguous	15.9 dB	28 V	16.7 dBm	1 %	–

cables are required to connect both prototypes. A future version of the demonstrator would integrate the RF components on the back side of the antenna ground plane.

A console was developed in order to manage both prototypes simultaneously. Depending on the active CA configuration, the reconfigurable RF front-end is programmed with the appropriate frequencies. Furthermore, the LTE band 20 PA is only

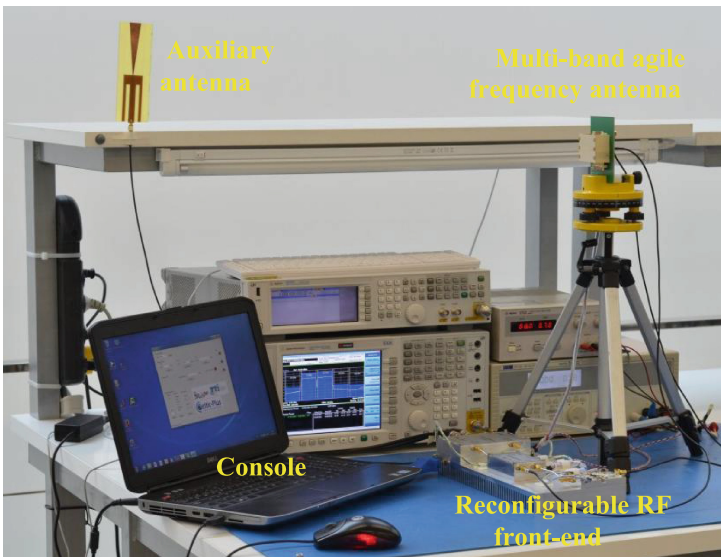


**Fig. 10.** Reconfigurable CA demonstrator.

activated in inter-band CA configuration to save energy during intra-band CA. In the multi-band frequency agile antenna, the DTCs are also programmed to tune the antenna resonances properly.

To validate both prototypes, a second antenna emulating the user equipment antenna was used to perform a radio link as shown Fig. 10.

Different CA configurations were performed combining both prototypes. Figure 11 shows one example of the test results at the auxiliary antenna with 2CCs in intra-band contiguous CA configuration. The demonstrator proves the ability of both prototypes to support CA.



**Fig. 11.** Test results from the reconfigurable CA demonstrator at the auxiliary antenna for 2CCs in intra-band contiguous CA.

## 5 Conclusions

In this contribution, energy efficiency miniaturized dual band LTE small cell base station using CA for capacity network improvement is demonstrated.

The dual band reconfigurable RF front-end supports CA up to 3 CCs and provides energy saving up to 50 % using different operating points depending on the active CA configuration. It supports intra-band contiguous and non-contiguous CA as well as inter-band CA. The dual band antenna system, developed in parallel with the RF front-end, is capable to adapt its frequency bandwidth according to the RF front-end configuration (CA mode). This frequency bandwidth optimization has led to a miniaturization of the antenna system by a factor 3 without impacting its electrical performance.

The measured performances of both sub-systems are analyzed and a reconfigurable CA demonstrator combining the RF front-end and the antenna system is presented.

**Acknowledgments.** The present work was carried out within the framework of Celtic-Plus SHARING project.

## References

1. Zukang, S., Papasakellariou, A., Montojo, J., Gerstenberger, D., Fangli, Z.: Overview of 3GPP LTE-advanced carrier aggregation for 4G wireless communications. *IEEE Commun. Mag.* **50**, 122–130 (2012)
2. Avser, B., Rebeiz, G.M.: Low-profile 700–970 MHz and 1600–2200 MHz Dual-band tunable antenna for carrier aggregation systems. In: *IEEE Antennas and Propagation Society International Symposium (APSURSI)* (2014)
3. Best, S.: Optimization of the bandwidth of electrically small planar antennas. In: *Antenna Applications Symposium*, Monticello, IL (2009)
4. Sievenpiper, D.F., Dawson, D.C., Jacob, M.M., Kanar, T., Kim, S., Long, J., Quarfoth, R.G.: Experimental validation of performance limits and design guidelines for small antennas. *IEEE Trans. Antennas Propag.* **60**(1), 8–19 (2012)
5. Jouanlanne, C., Delaveaud, C.: Compact dual-band frequency agile antenna designed for carrier aggregation LTE small cell. In: *20th International Symposium on Wireless Communication Systems* (2015)
6. 3GPP TR36.104, Release 12: Base Station Radio Transmission and Reception (2015)
7. Kowlgi, S., Berland, C.: Linearity considerations for multi-standard cellular base station transmitters. In: *European Microwave Conference*, pp. 226–229 (2011)
8. 3GPP TR36.141 Release 12: Base Station Conformance Testing (2015)